Effects of Chemical Modifications on Photophysics and Exciton Dynamics of π-Conjugation Attenuated and Metal-Chelated Photoconducting Polymers

L.X. Chen*[a], W.J.H. Jäger[a], D.J. Gosztola[a], M.P. Niemczyk[a] and M.R. Wasielewski[a,b]
[a]Chemistry Division, Argonne National Laboratory, Argonne, Illinois 60439
[b]Department of Chemistry, Northwestern University, Evanston, Illnois 60208

Abstract

Effects of two types of chemical modifications on photoconducting polymers consisting of polyphenylenevinylene (PPV) derivatives are studied by static and ultrafast transient optical spectroscopy as well as semi-empirical ZINDO calculations. The first type of modification inserts 2,2'-bipyridyl-5-vinylene units (bpyV) in the PPV backbone, and the second type involves metal -chelation with the bpy sites. Photoluminescence and exciton dynamics of polymers **1** and **2** with PV:bpyV ratios of 1 and 3 were examined in solution, and compared to those of the homo-polymer, poly(2,5-bis(2'-ethylhexyloxy)-1,4-phenylenevinylene) (BEH-PPV). Similar studies were carried out for several metal-chelated polymers. These results can be explained by changes in π-conjugation throughout the polymer backbone. The attenuation in π-conjugation by the chemical modifications transforms a conducting polymer from one-dimensional semiconductor to molecular aggregates.

Keywords

poly(phenylene vinylene) derivatives, molecular aggregates, π-conjugation, time-resolved fast spectroscopy, chemical synthesis, semi-empirical and model calculations.

Introduction

In order to expand applications for conducting polymers, chemical modifications have been carried out by researchers[1-6]. These modifications may occur at the backbone or at the side groups of the polymers[5,7-10]. In this study, the photophysics of two poly(phenylene vinylene) (PPV) derivatives which are chemically modified at the backbone (Figure 1), is investigated. Two types of chemical modifications have been carried out, (1) inserting bpyV between every one and three phenylene vinylene (PV) units, and (2) chelating metal ions at these bpyV sites[3]. The first modification introduces a π-conjugation attenuator, bpyV, prompting nonplanar conformation along the backbone because the rotation barrier along the C-C bond connecting two pyridine rings is very small[11]. The second modification introduces restrictions to the C-C bond rotation as well as metal electrons interacting with the polymer. Because these modifications alter electronic structures of conjugated polymers, functions of the polymers based on the photoinduced electron transfer and photoluminescence are changed. Our understanding of the origins for the effects brought upon by chemical modifications allows rationally design photoconducting polymers for various applications. In this report, we combine optical characterization, structural determination and semi-empirical quantum mechanical calculations[12,13] to establish structure/function relationships of the polymers and the interplay of different factors that determine the properties.

Samples and Methods

Synthesis of the polymers in Figure 1 was described elsewhere[3]. All measurements were conducted in toluene solutions at room temperature. Metal-chelated polymers were formed by

adding stoichiometric amounts of methanol solutions of metal ions to give metal:bpy =1:1, or as otherwise indicated. Experimental setups for transient optical absorption and time-resolved fluorescence measurements were reported previously[12,13].

Results and Discussions

1. Effects of Inserting bpyV into Polymers 1 and 2

Because of the rotations along the C-C bond in the bpy groups mentioned above, the planar conformation of a conjugated polymer backbone is interrupted, resulting in a weakened π-conjugation. This effect is more significant in polymer **1** than in polymer **2**. The π-conjugation attenuation causes progressive blue shifts of the absorption peaks, enhancements of photoluminescence (PL) quantum yields (Figure 2), as well as an increasing excitation wavelength λ_{ex} dependence in the transient absorption spectra (Figure 3). When well-conjugated BEH-PPV was excited at blue and red sides of the lowest energy absorption peak, little difference was observed in the shapes of the transient optical spectra which resemble the PL spectrum in the stimulated emission (SE) region (530-630 nm). However, the blue and red excitations for polymer **2** result differently, with only the latter resembling the PL spectrum in the SE region. When all the polymers were excited by 417 nm light at the blue side of the absorption peaks, the transient absorption of BEH-PPV had only an amplitude decay, but those for polymer **2** and **1** exhibited spectral shifts, shape changes as well as the amplitude decays, with a slower rate, a larger shift and a more drastic change in shape for the latter (not shown). The excited state populations monitored via the photoinduced absorption in the near IR region (e.g. 750 nm) for the three polymers (Figure 4) show that BEH-PPV has the shortest lifetime while polymer **1** not only has the longest lifetime, but also has a rising component after the excitation (see inset). Moreover, the fluorescence lifetimes for polymers **1** and **2** are also extended due to the π-conjugation attenuation. To summarize, we observed systematic changes in photophysical behaviors among the polymers due to π-conjugation attenuation and these effects have been confirmed by sequential comparisons among the three polymers.

Based on the observations mentioned above, PPV type polymers in solution can be described as an ensemble of interacting oligomers. The electronic coupling between the oligomers determines the strength for the π-conjugation, and the photophysics of the polymer. Attenuation of the coupling between the oligomers can be introduced by structural distortions from a planar conformation of the backbone within an oligomeric segment, or an electronic structural mismatch between adjacent monomers. The bpy groups in polymers **1** and **2** accomplish both, causing quantum confinements in the polymers (Figure 5). BEH-PPV with strongly interacting oligomers facilitates high mobilities for the initial excitons and charge carriers, leading to effective formation of non-emissive species as well as fast exciton relaxation to the emissive exciton state. Therefore, BEH-PPV has a shorter excited state lifetime and lower PL efficiency. Polymers **1** and **2** with attenuated π-conjugation and barriers for the excitons and charge carriers along the chain have (1) slower rates for initial excitons to relax to the final emissive exciton, and (2) lower mobilities for charge carriers to diffuse to non-emissive species. Therefore, the quantum confinement due to the attenuated π-conjugation by the bpy groups inserted in the conjugated polymer backbone are the origins for a series of changes in the photophysical properties, such as the longer lifetimes of the excited states, the slower spectral diffusion and the higher PL quantum yields, compared to BEH-PPV. Based on our study, a correlation between the π-conjugation and photophysics in conjugated

DISCLAIMER

DISCLAIMER

Portions of this document may be illegible in electronic image products. Images are produced from the best available original document.

polymers in solutions can be established. When the π-conjugation is strong, the photophysics of the polymer is similar to that for a one-dimensional semiconductor; when the π-conjugation is weakened, the polymer is better represented as a string of chromophores[14-17]. The balance between PL efficiency and charge carrier mobilities is important in designing new materials for the photonics applications.

2. Effects of Metal Chelation to Polymer 1 and 2

Comparing metal-free polymers **1** and **2**, two possible structural changes occur in metal-chelated polymers, (1) restricting the C-C bond rotation, and (2) metal electron participation in the polymer backbones. When a bidentate metal-chelation (which was confirmed by our other studies[13]) is formed, the planar conformation of the backbone and the π-conjugation should be re-established. Therefore, red-shifts in the lowest energy absorption peaks for metal-chelated polymers are expected and shown in Figure 6. However, some questions remain: (1) red-shifted absorption peaks are at lower energies than those in well-conjugated BEH-PPV, (2) the magnitudes of the red-shifts in polymer **1** are greater than those in polymer **2**, and (3) the red-shifts are metal specific, the ionochromic effect. These phenomena suggest that restoring the planar conformation of the backbone is not the only reason for the red-shifts.

PL spectra of the metal-chelated polymers also exhibit ionochromic effects, depicted in Figure 7 for Zn(II)- and Ni(II)- chelated polymer **2**. However, their PL behaviors are completely different. The former has a dual emission for metal-free and Zn(II)-chelated polymer, respectively. When λ_{ex} is at 550 nm, only the Zn(II)-chelated polymer absorbs, so the PL spectrum has a broad single peak, red-shifted from that of the metal-free polymer **2** (Figure 2). As λ_{ex} becomes shorter in wavelength, the PL spectra can be decomposed into those from the metal-free and from the Zn-chelated polymer **2**. The Ni(II)-chelated polymer **2** shows the PL features only from the metal-free polymer. When λ_{ex} is at 570 nm where only a Ni(II)-chelated polymer absorbs, no PL was detected. The PL of Ni(II)-chelated polymer is significantly quenched. The excited state and the average PL lifetimes of metal-chelated polymer **2** (not shown) are metal dependent. For close-shell Zn(II)-chelated polymer **2**, the excited state lifetime, the PL lifetime and the quantum yield increase 30%, 100% and 50% respectively, compared to the metal-free polymer. However, open-shell Ni(II) and Fe(III)-chelated polymers reduce the average excited state and the PL lifetimes by more than an order of magnitude compared to that of the metal-free polymer. The PL decays of various polymer **2** with and without metal-chelation can be described by biexponential functions, with a fast component which is metal-dependent, ranging from a few ps to several hundred ps, and a slow component which is metal-independent, with a time constant near 2 ns (Figure 8). The long component for the metal-free polymer **2** is about 1ns. The variation of the average lifetimes for the excited states and the PL for different metal-chelated polymers is due to changes in the relative ratio between the short and the long components, but the values of the time constants for the long components are unchanged and metal-independent.

Based on a series of structural and dynamics studies[13] which are not detailed here due to the limit in the scope of the paper, photophysical properties of metal-chelated polymers **1** and **2** can be explained by their dual properties as metal-chelated, conjugated polymers, and as metal-bpy complexes with extended π-conjugated ligands[18]. The electronic interactions between the metal and the polymers were modeled through a series of ZINDO calculations for metal-free, Zn(II)- and Ni(II)-chelated fragments resembling the polymers[19], and the energy levels of molecular orbitals (MOs) for these fragments are shown in Figure 9. The calculations show that the participation of

electrons from metal ions lowered energy levels for frontier MOs globally through both σ and π bonding, resulting in smaller enery gaps for the π-π* transition, thus, in the red-shifts in the lowest energy absorption peaks. The differences in the electronic structures of the metal ions produce the ionochromic effects. As more PV units are attached to the metal-chelated fragments in the calculations, energy levels of the MOs have a tendency to approach those of the metal-free fragments, showing the interplay between the metal-chelation and the extended PV fragments. The drastic lowering of the energy levels for the MOs suggests that although the bidentate metal-chelation restores the planar conformation of the backbone, it introduces potential barriers due to structural incompatibility between the metal complexes and the PV units, causing the quantum confinement of excitons. Thus, despite a planar conformation in the backbone, the π-conjugation along the backbone for close-shell Zn(II)-chelated polymer **2** is actually weakened compared to the metal-free polymer, signaled by a longer lifetime for the excited state and the PL, as well as a higher PL yield. However, for open-shell metal ions with the spin-orbit couplings as well as the metal-to-ligand-charge-transfer (MLCT) transitions, the PL and the excited state dynamics of metal-chelated polymers follow a trend parallel to their counterparts of simple bpy complexes, with short excited state lifetimes and quenched PL resulting from non-radiative decay of the excitons. Thus, close-shell metal-chelated polymers represent a case that photophysics is still dominated by the π-π* transition affected by the metal-chelation, whereas the open-shell metal-chelated polymers represented an exciton dynamics that is dominated by MLCT transitions and spin-orbit couplings. Regarding potential applications, the close-shell metal-chelated polymer **2** could be used to manipulate the absorption and emission spectra and to enhance the PL quantum efficiency, while the open-shell metal-chelated polymers may have applications in metal ion sensing.

Acknowledgement

This work was supported by the Environmental Management Science Program and by the Division of Chemical Sciences, Office of Basic Energy Sciences, U. S. Department of Energy under contract W-31-109-Eng-38. The authors would like to thank Professors Frank Spano, Lewis Rothberg, and Russell H. Schmehl for their helpful discussions and Dr. Eric S. Manas for his help in ZINDO calculations.

Figure Captions

1. Structures of metal-free and metal-chelated polymers.
2. Absorption (left) and emission (right) spectra of the polymers. The emission spectra have been corrected, so the areas under the spectra are proportional to the PL quantum yields.
3. λ_{ex} dependence of transient absorption spectra for (a) BEH-PPV and (b) polymer **2** plotted along their absorption and PL spectra. The middle region (530-630nm) is the SE region. The left of that monitors the ground state bleaching and the right, the excited state absorption.
4. The excited state decay dynamics monitored in the near IR region (~750 nm) for the polymers. The inset displays the dynamics in the early times after the excitation, where a rising component was observed in π-conjugation attenuated polymer **1**.
5. Potential barriers along the polymer backbone due to the bpy groups, showing the quantum confinement that prevents the excitons diffusing into distant polarons along the polymer chain.
6. Absorption spectra of metal-chelated polymer **1** (a) and polymer **2** (b) along with the absorption spectra of their parent metal-free polymer and of BEH-PPV.

7. PL spectra for partially Zn(II)-chelated (a) and Ni(II)-chelated (b) polymer **2**.
8. PL decays of metal-chelated polymers excited at 402 nm and monitored at wavelengths indicated.
9. Energy levels of MOs for molecular fragments of three series vs. the number of the PV units, n, attached. In metal-free fragments, energies for the HOMOs and the LUMOs change with n in a symmetric way, whereas metal-chelated fragments show a global lowering of the energy levels for the MOs and a tendency of approaching to the energy distributions of the metal-free fragments.

References

1)Ley, K. D.; Whittle, C. E.; Bartberger, M. D.; Schanze, K. S. *J. Am. Chem. Soc.* **1997**, *119*, 3423-3424.
2)Ley, K. D.; Walters, K. A.; Schanze, K. S. *Synth. Met.* **1999**, *102*, 1585-1586.
3)Wang, B.; Wasielewski, M. R. *J. Am. Chem. Soc.* **1997**, *119*, 12-21.
4)Yamamoto, T.; Yoneda, Y.; Maruyama, T. *J. Chem. Soc., Chem. Commun.* **1992**, 1652-4.
5)Peng, Z.; Gharavi, A. R.; Yu, L. *J. Am. Chem. Soc.* **1997**, *119*, 4622-4632.
6)Yamamoto, T.; Hayashida, N.; Maruyama, T.; Kubota, K. *Chem. Lett.* **1998**, 1125-1126.
7)Harvey, P. P.; Fortin, D. *Coord. Chem. Rev.* **1998**, *171*, 351-354.
8)Chan, W. K.; Gong, X.; Ng, W. Y. *Appl. Phys. Lett.* **1997**, *71*, 2919-2921.
9)Peng, Z.; Yu, L. *J. Am. Chem. Soc.* **1996**, *118*, 3777-8.
10)Segawa, H.; Wu, F. P.; Nakayama, N.; Maruyama, H.; Sagisaka, S.; Higuchi, N.; Fujitsuka, M.; Shimidzu, T. *Synth. Met.* **1995**, *71*, 2151-4.
11)Galasso, V.; De Alti, G.; Bigotto, A. *Tetrahedron* **1971**, *27*, 991.
12)Chen, L. X.; Jaeger, W. J. H.; Niemczyk, M. P.; Wasielewski, M. R. *Effects of pi.-Conjugation Attenuation on the Photophysics and Exciton Dynamics of Poly(p-phenylenevinylene) Polymers Incorporating 2,2'-Bipyridines*, 1999; Vol. 103, pp 4341-4351.
13)Chen, L. X.; Jager, W. J. H.; Gosztola, D. J.; Niemczyk, M. P.; Wasielewski, M. R. *Journal of Physical Chemistry, B* **2000**, *104*, Web release, Feb.4, 2000.
14)Sariciftci, N. S. *Primary Photoexcitations in Conjugated Polymers: Molecular Exciton Versus Semiconductor Ban Model*, 1997.
15)Conwell, E. *Primary Photoexcitations Conjugated Polym.* **1997**, 99-114.
16)Yan, M.; Rothberg, L. J.; Papadimitrakopoulos, F.; Galvin, M. E.; Miller, T. M. *Phys. Rev. Lett.* **1994**, *72*, 1104-7.
17)Bassler, H. *Primary Photoexcitations Conjugated Polym.* **1997**, 51-98.
18)Strouse, G., F., ; Schoonover, J. R.; Duesing, R.; Boyde, S.; Jones, J., W. E., ; Meyer, T. J. *Inorganic Chemistry* **1995**, *34*, 473.
19)Manas, E.; Chen, L. X. *unpublished results.* **2000**.

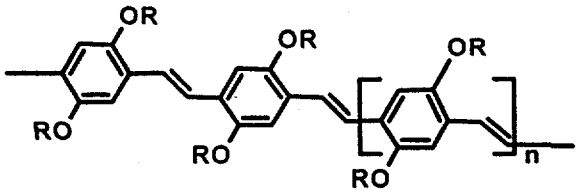

BEH-PPV

R=

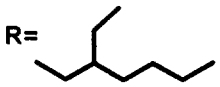

2-ethyl-hexyl

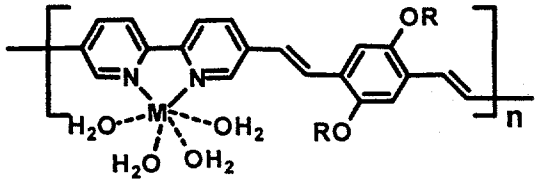

Polymer 1 + metal

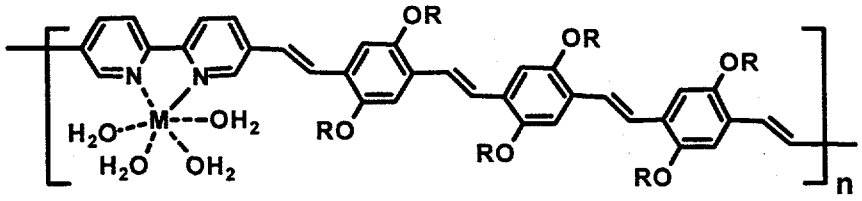

Polymer 2 + metal

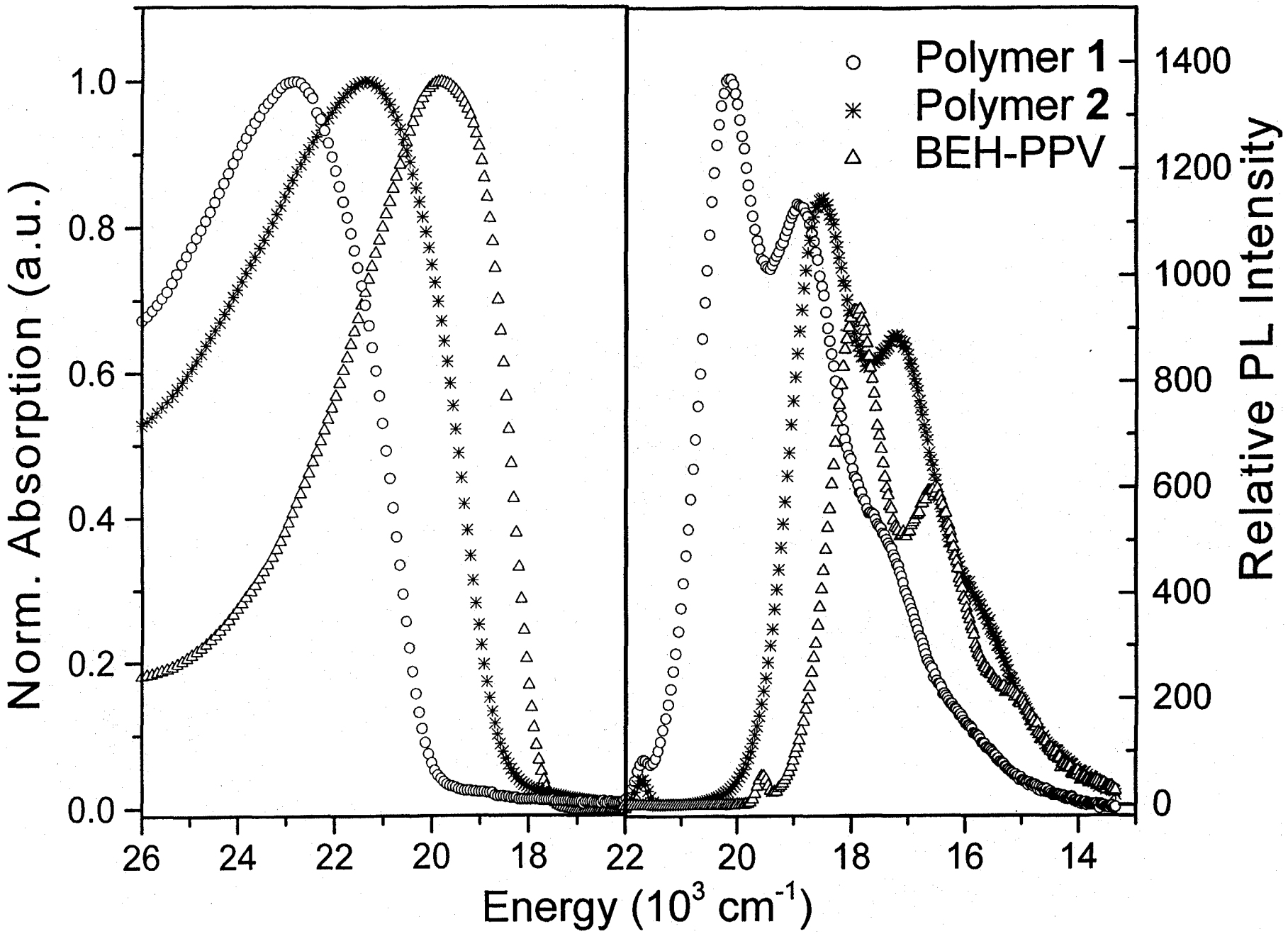
Polymer 1
Polymer 2
BEH-PPV
Norm. Absorption (a.u.)
Relative PL Intensity
Energy (10^3 cm^{-1})
0.0
0.2
0.4
0.6
0.8
1.0
0
200
400
600
800
1000
1200
1400
26
24
22
20
18
22
20
18
16
14

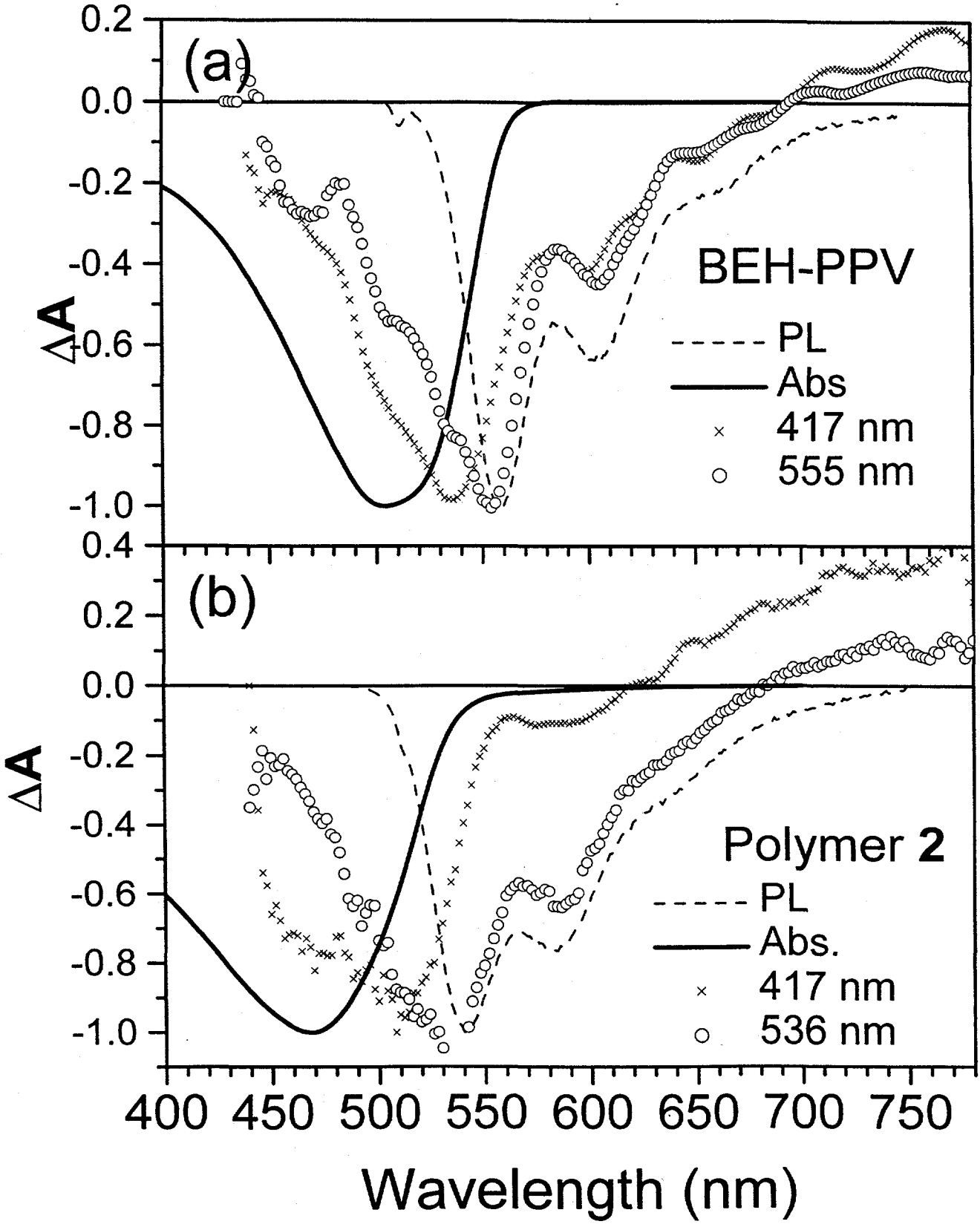
(a)
BEH-PPV
PL
Abs
417 nm
555 nm
ΔA
(b)
Polymer 2
PL
Abs.
417 nm
536 nm
ΔA
Wavelength (nm)

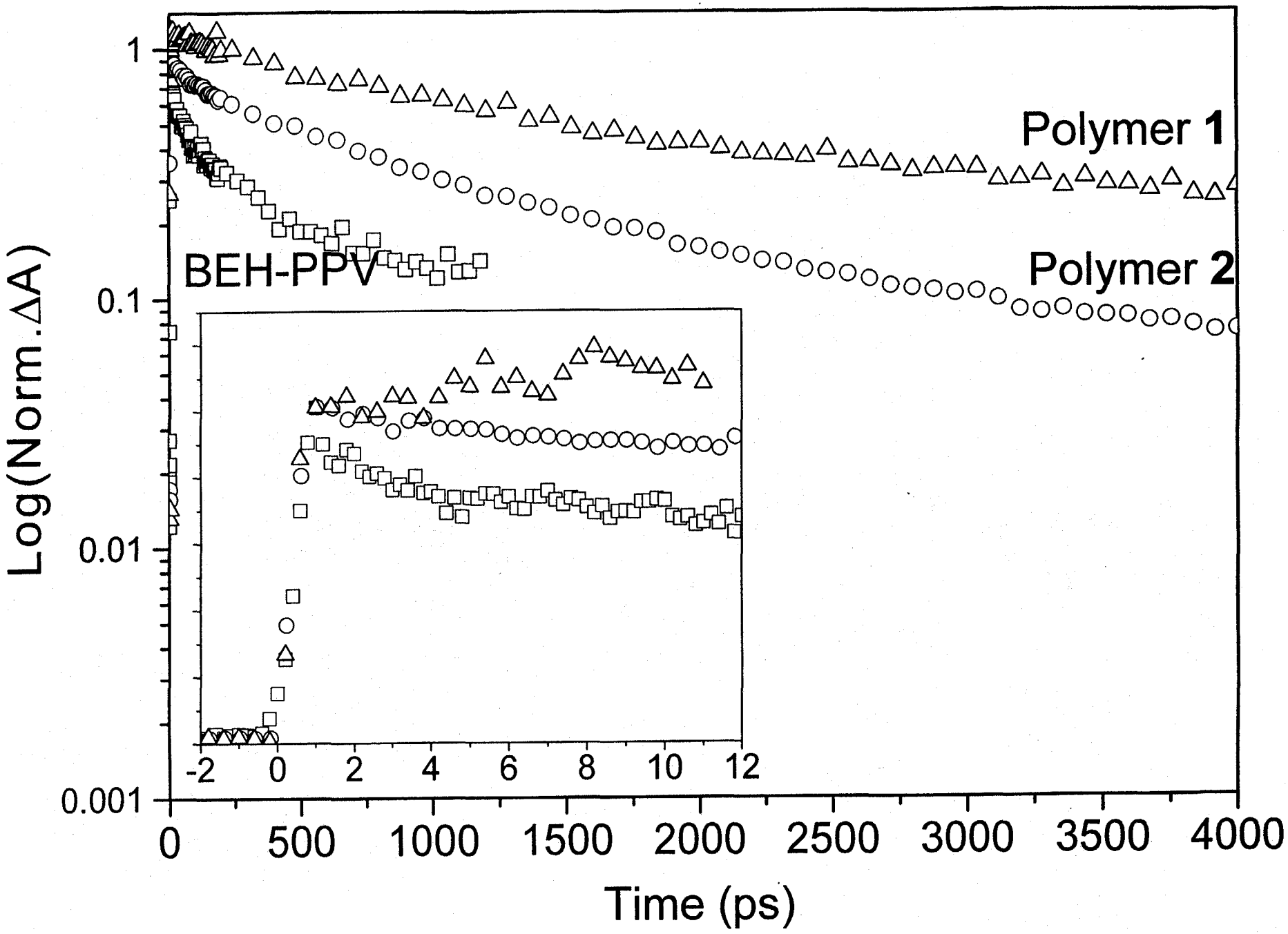
Polymer 1
Polymer 2
BEH-PPV
Log(Norm.ΔA)
Time (ps)
1
0.1
0.01
0.001
0
500
1000
1500
2000
2500
3000
3500
4000
-2
0
2
4
6
8
10
12

Fig.

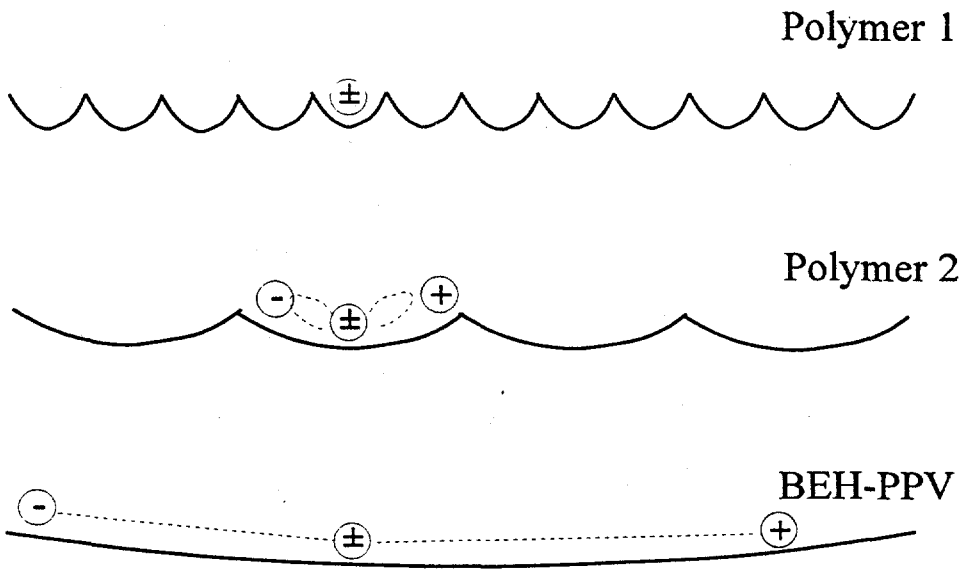
Polymer 1
Polymer 2
BEH-PPV

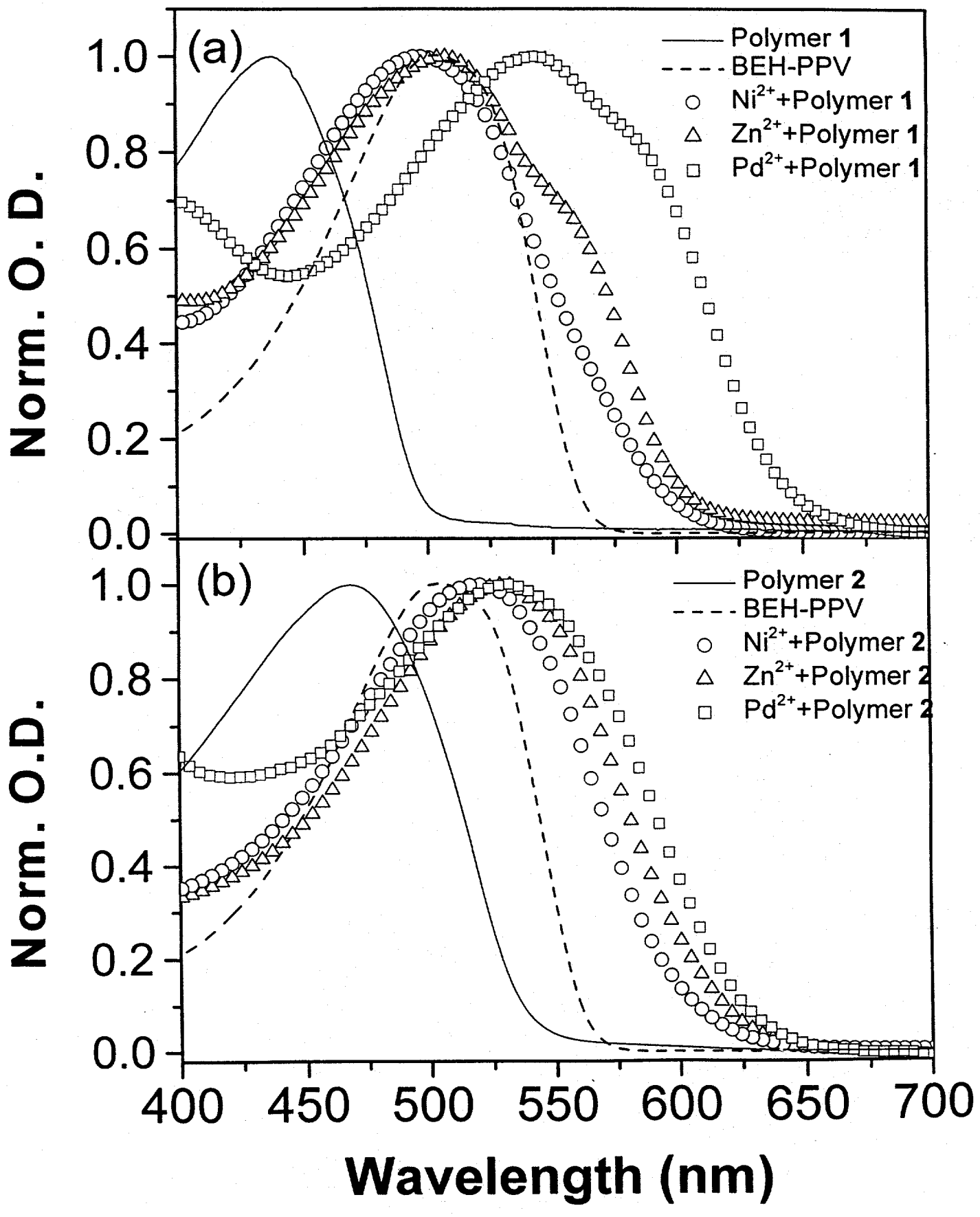
(a)
Polymer 1
BEH-PPV
Ni2+ +Polymer 1
Zn2+ +Polymer 1
Pd2+ +Polymer 1
Norm. O. D.
1.0
0.8
0.6
0.4
0.2
0.0
(b)
Polymer 2
BEH-PPV
Ni2+ +Polymer 2
Zn2+ +Polymer 2
Pd2+ +Polymer 2
Norm. O.D.
1.0
0.8
0.6
0.4
0.2
0.0
400
450
500
550
600
650
700
Wavelength (nm)

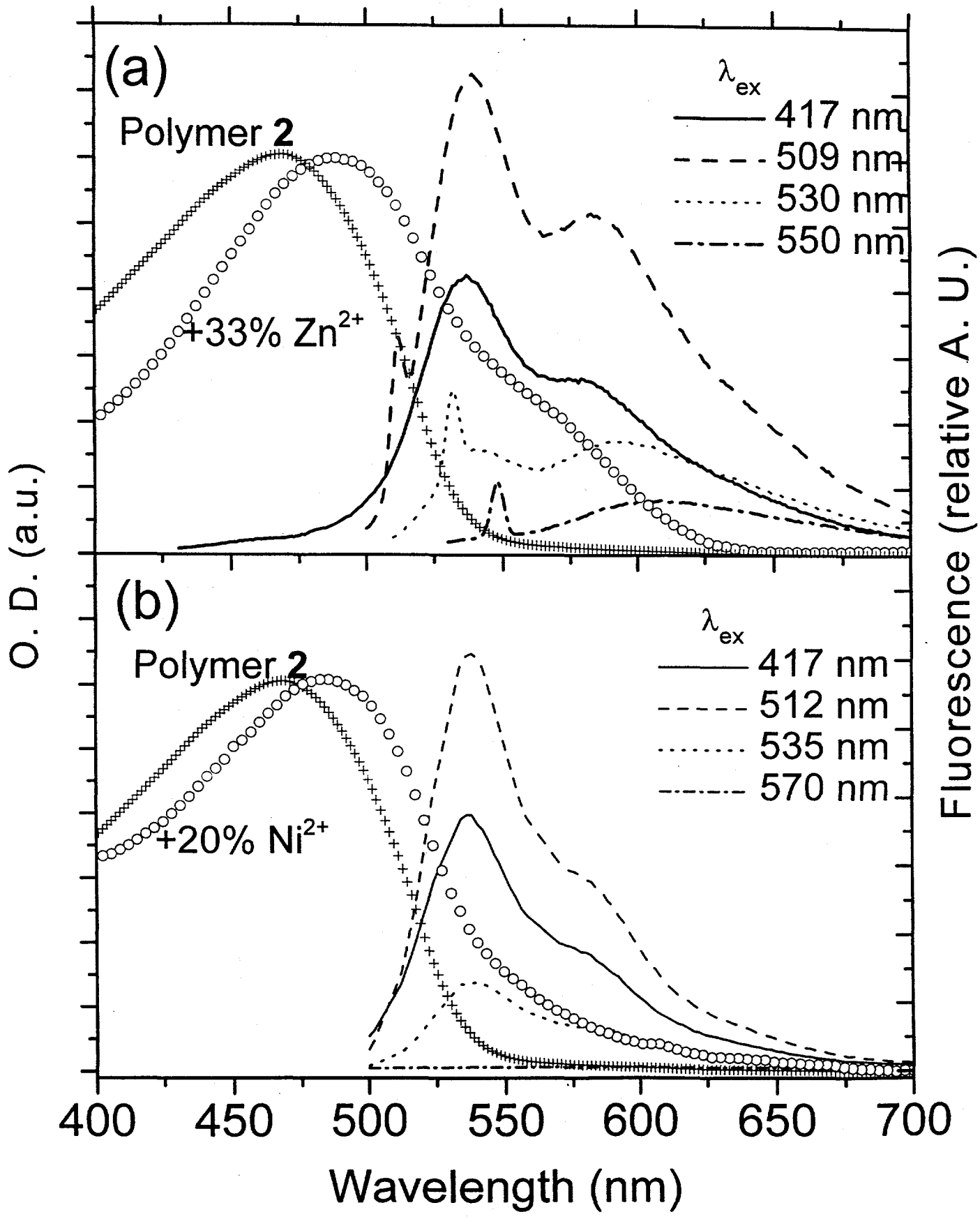
(a)
Polymer 2
+33% Zn2+
λex
417 nm
509 nm
530 nm
550 nm
(b)
Polymer 2
+20% Ni2+
λex
417 nm
512 nm
535 nm
570 nm
O. D. (a.u.)
Fluorescence (relative A. U.)
400
450
500
550
600
650
700
Wavelength (nm)

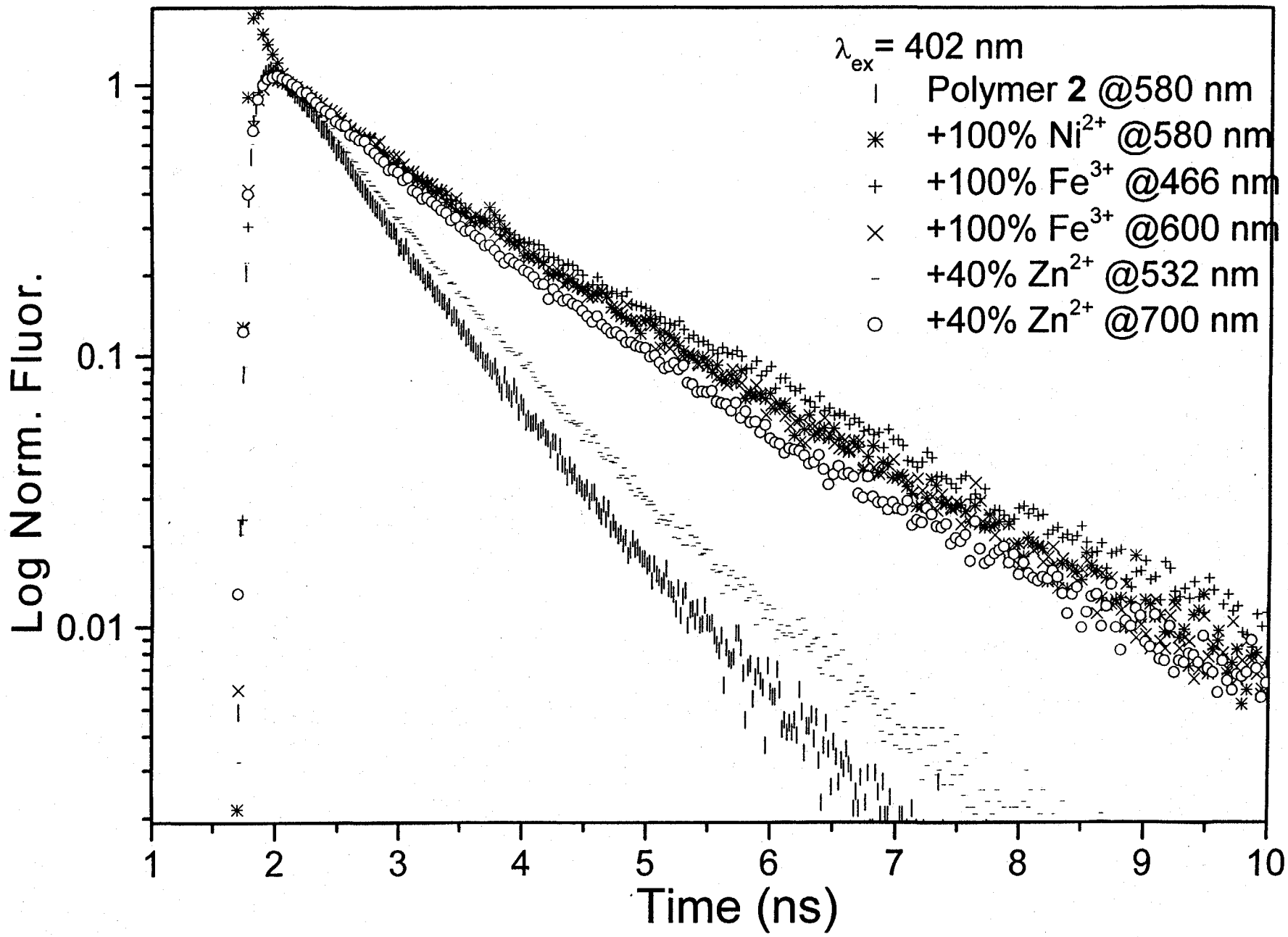
λ_{ex} = 402 nm
Polymer **2** @580 nm
+100% Ni^{2+} @580 nm
+100% Fe^{3+} @466 nm
+100% Fe^{3+} @600 nm
+40% Zn^{2+} @532 nm
+40% Zn^{2+} @700 nm
Log Norm. Fluor.
1
0.1
0.01
1
2
3
4
5
6
7
8
9
10
Time (ns)

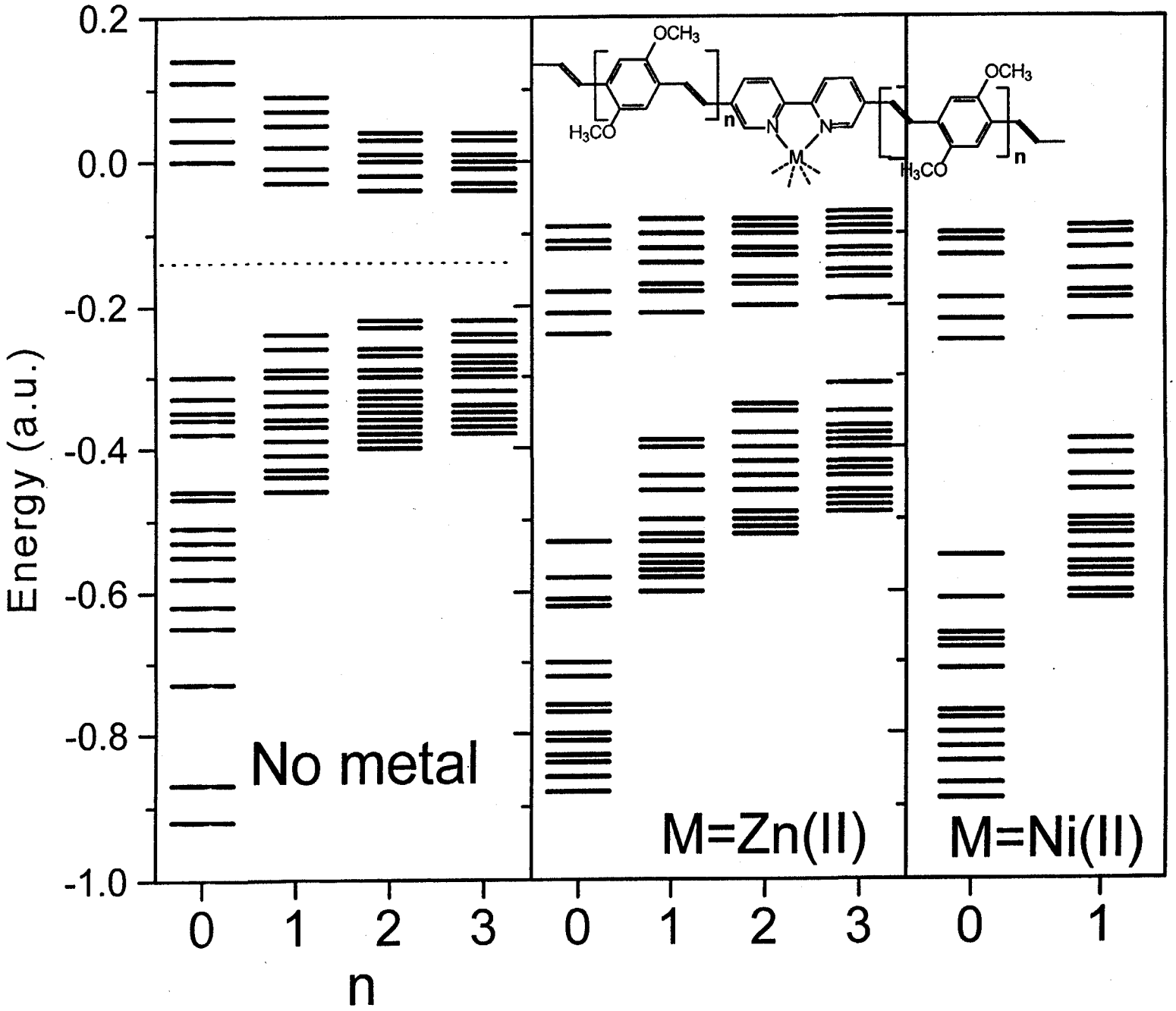
0.2
0.0
-0.2
-0.4
-0.6
-0.8
-1.0
Energy (a.u.)
No metal
M=Zn(II)
M=Ni(II)
0
1
2
3
0
1
2
3
0
1
n
OCH3
H3CO
n
N
N
M
OCH3
H3CO
n

Fig. 9.